A method to obtain uniform magnetic-field energy density gradient distribution using discrete pole pieces for a microelectromechanical-system-based magnetic cell separator

Pulak Nath[a)]
Biomedical Engineering, The Cleveland Clinic Foundation, Cleveland, Ohio 44195 and Department of Chemical and Biomedical Engineering, Cleveland State University, Cleveland, Ohio 44115

Lee R. Moore, Maciej Zborowski, Shuvo Roy, and Aaron Fleischman
Biomedical Engineering, The Cleveland Clinic Foundation, Cleveland, Ohio 44195

(Presented on 3 November 2005; published online 24 April 2006)

A spatially uniform magnetic energy density gradient ($\nabla \mathbf{B}^2$) distribution offers a controlled environment to separate magnetically tagged cells or biomolecules based on their magnetophoretic mobility [L. R. Moore *et al.*, J. Biochem. Biophys. Methods **37**, 11 (1998)]. A design to obtain a uniform ∇B^2 distribution for a microelectromechanical-systems-based magnetic cell separator was developed. The design consists of an external magnetic circuit and a microfabricated channel (biochip) with embedded discrete pole pieces on the channel walls. The two-dimensional and three-dimensional magnetostatic simulation softwares utilizing boundary element methods were used to optimize the positions and the dimensions of the discrete pole pieces, as well as the external magnetic circuit—the combination of which would generate a uniform $\nabla \mathbf{B}^2$ profile over the channel cross section. It was found that the discrete pole pieces required specific magnetic properties (saturation magnetization constant >1.55 T) to affect the overall $\nabla \mathbf{B}^2$ distribution. Investigating different positions of the discrete pole pieces inside the external magnetic field indicated that the proposed design could generate uniform $\nabla \mathbf{B}^2$ distribution with ± 100 μm displacements along the height/width and $\pm 1°$ inclination from the optimum position. © *2006 American Institute of Physics*.
[DOI: 10.1063/1.2171936]

INTRODUCTION

Magnetic cell separation techniques are becoming increasingly popular in biomedical applications due to their high sensitivity, selectivity, and ease of operation.[1] However, magnetic separation applied to biology is an emerging technology and applications of magnetic fields to separate cells are being refined constantly[2–6] to meet the demands of high efficiency, automation, and low costs.

A force balance on the particle suspended in a fluid flowing through a magnetic field can retrieve the expression for cell migration velocity in terms of the magnetic properties of the particle, medium, and the magnetic field, and is as follows:[2]

$$\boldsymbol{\nu} = \frac{2R^2 \Delta\chi}{9\eta} \nabla \left(\frac{B^2}{2\mu_0} \right), \tag{1}$$

where $\boldsymbol{\nu}$ is the magnetic migration velocity of the particle, η is the fluid viscosity, R is the particle radius, V is the cell volume, $\Delta\chi$ is the cell volumetric susceptibility relative to medium, μ_0 is the permeability of free space, and $\nabla(B^2/2\mu_0)$ is the magnetostatic energy density gradient. Equation (1) indicates that the velocity of a particle in a suspended media induced by the external magnet is directly proportional to $\nabla \mathbf{B}^2$. Common magnetic cell sorters such as the high gradient magnetic cell sorters (HGMSs) use a high gradient to magnetically trap cells within the separation column irrespective of their differential magnetic susceptibilities. In contrast, the ability to fractionate cells based on their differential magnetic susceptibilities has significant clinical relevance. Fractionation of cells for such applications can be obtained by using an isodynamic open-gradient magnetic field extended over a relatively large volume of flow.[2] Therefore, a uniform $\nabla \mathbf{B}^2$ profile throughout the flow path of the cells is an important requirement for fractionating cells based on their differential magnetic properties. Nonplanar dipoles such as hyperbolic-shaped pole pieces have been used to provide uniform $\nabla \mathbf{B}^2$ distribution on the separation zone for continuous magnetic separation of particles according to their magnetic susceptibilities.[2,7] In addition to a uniform $\nabla \mathbf{B}^2$ distribution, the flow in the separation zone must also be laminar and orthogonal to the field gradient. Laminar flow is an intrinsic property of microelectromechanical-systems-(MEMS) based microfluidic devices, and therefore microfabricated channels are ideal for the development of an isodynamic open-gradient magnetic cell sorter. However, microfabrication technologies are generally implemented on planar structures. Consequently, a planar magnetic design is required for such MEMS- based magnetic cell sorters. In this paper, a magnet design composed of planar discrete pole pieces and an external permanent magnet assembly is presented that is capable of providing a uniform $\nabla \mathbf{B}^2$ over a certain region.

[a)]Electronic mail: nathp@ccf.org

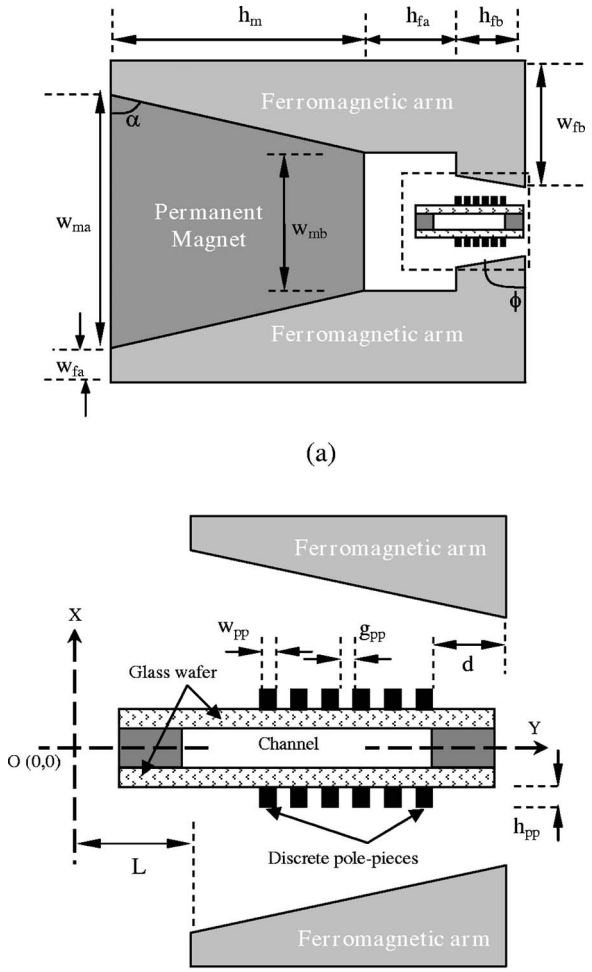

FIG. 1. (a) Schematic cross-section diagram (not to scale) showing the external magnetic circuit. (b) Schematic cross-section diagram (not to scale) showing the biochip with embedded discrete pole pieces. (The direction of the fluid flow is perpendicular to the plane of the cross section.)

MODEL DESCRIPTION

A schematic illustration of the magnetic circuit is presented in Fig. 1. The magnetic circuit is composed of two major sections:

(1) a trapezoidal external magnet assembly with ferromagnetic "arms" to form a defined gap between the dipoles, and
(2) a set of discrete pole pieces embedded on the sidewalls of a microfluidic chip (biochip) that will be positioned in the gap of the external circuit

The magnetic field and gradient of the proposed model were investigated using the two-dimensional (2D) and three-dimensional (3D) magnetostatic simulation softwares (MAGNETO and AMPERES, Integrated Engineering software, Manitoba, Canada) utilizing boundary element methods. An iterative approach was undertaken to vary different geometric parameters of the proposed design to obtain a uniform $\nabla \mathbf{B}^2$ profile over a desired region. In addition to finding a favorable position of the discrete pole pieces assembly,

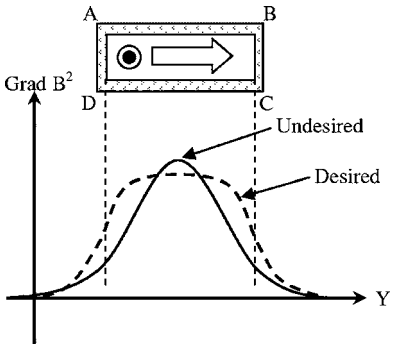

FIG. 2. Schematic diagram showing the desired and undesired magnitude of ∇B^2 distribution (indicated as GradB^2 in figures) along the cross section (ABCD) of the separation channel.

analysis of tolerance with respect to positioning the discrete pole pieces inside the gap of the ferromagnetic arms were also performed. Such analysis indicated the flexibility of the proposed design in terms of aligning the chip inside the gap.

The gap between the ferromagnetic poles was limited by the thickness of the microfluidic chip. The chip will be made of two 400-μm-thick glass wafers bonded together with 250-μm-deep channels in between the wafers, making the total thickness of the microfluidic chip to be 1050 μm. The discrete pole pieces will be fabricated on the outer walls of the chip. It was important to consider fabrication limitations for such approach before establishing the height (h_{pp}) of the pole pieces. Microfabricated films are often associated with stress mismatch and result in undesired effects such as poor adhesion, cracks, and wafer bowing. In this design, the height of the pole pieces was chosen to be 100 μm, with the assumption that this height would not encounter common fabrication problems associated with thick-film processing. Consequently, the final thickness of the chip was 1250 μm. The minimum gap (where the biochip will be placed) between the ferromagnetic arms was kept at 1800 μm so that the biochip can be inserted easily.

The desired $\nabla \mathbf{B}^2$ distribution in the separation channel is explained in Fig. 2 (magnitude of $\nabla \mathbf{B}^2$ distribution is indicated as GradB^2). ABCD represents the cross section of the channel at any point along the depth (Z, axis) of the channel. The flow is normal to the plane of the cross section. The direction of the magnetic force (represented by the block arrow) on a cell suspended in the flow needs to be along Y in order to move the cells laterally and thereby separate them from nonmagnetic cells. Therefore, the distribution of GradB^2 along Y (i.e., $\partial B^2/\partial Y$) needs to be uniform (as shown by the dashed curve) throughout the width of the channel cross section. For simplicity, all calculations were performed based on the $\nabla \mathbf{B}^2$ distribution along the midplane (i.e., $\partial B^2/\partial Y|_{x=0}$) of the proposed magnetic module. In general, a rectangular magnet would produce $\nabla \mathbf{B}^2$ distribution like the one presented by the solid curve in Fig. 2. Consequently, the top corner angle (ϕ) of the ferromagnetic arm in the external circuit and the numbers/size (w_{pp},h_{pp})/material, the gap between the pole pieces (g_{pp}), and the position (d) of the sets of discrete pole pieces were varied until uniform $\nabla \mathbf{B}^2$ distribution was obtained over a certain region.

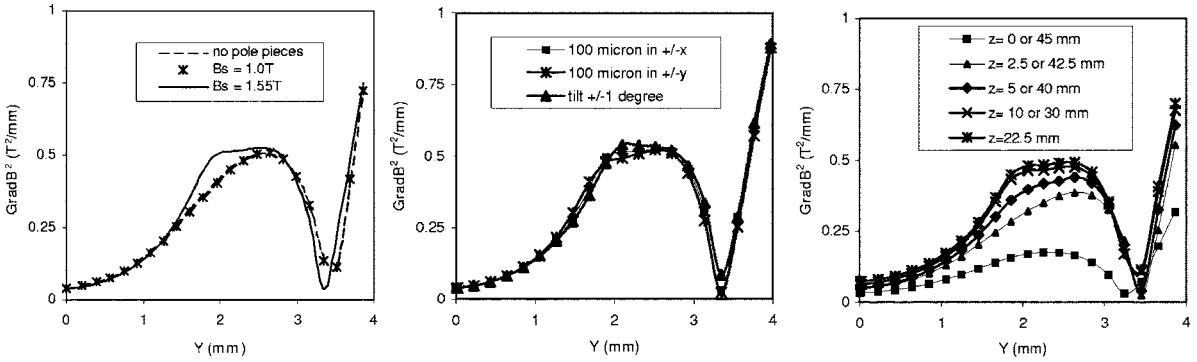

FIG. 3. (a) Graphs showing 2D simulation of GradB^2 profile of the proposed magnetic module with different pole-piece materials. (b) Graphs showing 2D simulation of GradB^2 profile with different misalignments in the x and y directions and different tilted positions from the midplane. (c) Graphs showing the 3D simulation of GradB^2 profile of the proposed magnetic module at different depths.

RESULTS AND DISCUSSIONS

Placing discrete pole pieces inside the magnetic field was able to further change the overall profile of the magnetic field. However, in order to obtain this change in the overall profile the saturation magnetization constant (B_s) of the discrete pole pieces had to be >1.55 T. Permalloy (Ni20Fe80), which is the most common magnetic material used in MEMS application, has a saturation magnetization constant of ~ 1.0 T, and will not be suitable for this application. The $\nabla \mathbf{B}^2$ profiles with no discrete pole pieces and discrete pole pieces of the final geometry with materials of different B_s are presented in Fig. 3(a). It shows that discrete pole pieces made of materials with $B_s \sim 1.0$ T have the same profile as that of air. The final design consisted of six discrete pole pieces on each side of the channel with saturation magnetization constant ~ 1.55 T and was found to provide uniform GradB^2 profile over 800 μm of the channel width. Other dimensions for this design are presented in Table I.

Possible misalignment in placing the discrete pole pieces inside the magnetic field was also investigated. It was found that misaligning the discrete pole pieces ± 100 μm from the midplane or along d did not change the GradB^2 distribution significantly [Fig. 3(b)]. Furthermore, if the set of discrete pole pieces is rotated $\pm 1°$ with the midplane (Y axis, at $X=0$), the uniformity of GradB^2 is well maintained [Fig. 3(b)].

Finally, the 3D simulation of the magnetic field was obtained by simple extrusion of the final 2D design. The GradB^2 profiles along different depths of a 45-mm-deep magnetic module are shown in Fig. 3(c). The average GradB^2 value at the center (along the depth) of the magnetic module was not only found to be uniform but also had increased by $\sim 15\%$ from the maximum GradB^2 that can be obtained without discrete pole pieces. However, magnetic-flux loss near the edges along the depth of the magnet caused reduction in the magnitude of average GradB^2. Nevertheless, beyond 5 mm into the depth of the magnet from both the edges the loss was negligible.

TABLE I. Dimensions of the final design. (Nomenclatures are illustrated in Fig. 1).

Nomenclature	Dimensions
w_{ma}	18.0 mm
w_{mb}	6.0 mm
w_{fa}	1.0 mm
w_{fb}	9.1 mm
h_m	20.5 mm
h_{fa}	2.5 mm
h_{fb}	2.0 mm
L	2.0 mm
α	73.68°
ϕ	74°
d	625 μm
g_{pp}	185 μm
w_{pp}	75 μm

CONCLUSIONS

In an effort to obtain uniform $\nabla \mathbf{B}^2$ profile utilizing planar magnetic components for MEMS-based magnetic cell separation, a permanent magnet/discrete pole pieces assembly is presented. Analysis of the proposed design revealed that the discrete pole pieces need to be made of materials with $B_s > 1.55$ T. It was also shown that the design is sufficiently flexible in terms of alignment of the biochip inside the magnetic field, which is very promising to adapt a "slide in" cartridge approach for practical applications. Such a design is not only suitable for magnetic cell separations but also can be extended to other applications such as cell tracking velocimetry and other biomagnetic separation applications.

[1] I. Safarik and M. Safarikova, J. Chromatogr., B: Biomed. Sci. Appl. **722**, 33 (1999).
[2] L. R. Moore, M. Zborowski, L. Sun, and J. J. Chalmers, J. Biochem. Biophys. Methods **37**, 11 (1998).
[3] G. Blankenstein, *Scientific and Clinical Applications of Magnetic Carriers*, edited by U. R. S. Hafeli *et al.* (Plenum, New York, 1997), pp. 233–248.
[4] J.-W. Choi *et al.*, Biomed. Microdevices **3**, 191 (2001).
[5] D. W. Inglis, R. Riehn, R. H. Austin, and J. C. Strum, Appl. Phys. Lett. **85**, 5093 (2004).
[6] K. H. Han and A. B. Frazier, J. Appl. Phys. **96**, 5797 (2004).
[7] J. Y. Hwang, M. Takayasu, F. J. Friedlaender, and G. Kullerud, J. Appl. Phys. **55**, 2592 (1984).